

Vibration equations of the coupled torsional, longitudinal, and lateral vibrations of the propeller shaft at the ship stern

Jabbar Firouzi¹, Hassan Ghassemi¹✉, Karim Akbari Vakilabadi²

¹ Amirkabir University of Technology, Department of Maritime Engineering, Tehran, Iran
e-mail: firozi.jabbar56@gmail.com; gasemi@aut.ac.ir

² Imam Khomeini Marine University, Department of Mechanical Engineering, Nowshahr, Iran
e-mail: akbari.karim@gmail.com

✉ corresponding author

Key words: vibration equations, coupled vibration, shaft and propeller, added mass, ship stern, hydrodynamic coefficients

Abstract

A propeller shaft generally experiences three linear forces and three moments, the most important of which are thrust, torque, and lateral forces (horizontal and vertical). Thus, we consider 4DOFs (degrees of freedom) of propeller shaft vibrations. This paper is presented to obtain the vibration equations of the various coupled vibrations of the propeller shaft at the stern of a ship (including coupled torsional-axial, torsional-lateral, axial-lateral, torsional-axial, and lateral vibrations). We focused on the added hydrodynamic forces (added mass and added damping forces) due to the location of the propeller behind the ship. In this regard, the 4DOFs of the coupled vibration (torsional-longitudinal and lateral vibrations in the horizontal and vertical directions) equations of shaft and propeller systems located behind a ship were extracted with and without added mass and damping forces. Also, the effect of mass eccentricity was considered on vibrations occurring at the rear of the ship.

Introduction

Vibrations occurring in marine propulsion systems significantly affect a ship's hydrodynamic performance, structure, noise propagation, and can cause a variety of problems. A ship propeller is often a source of vibration, and noise is transmitted through the shaft to a power transmission system and then farther into the ship. Propeller shafts experience different exiting loads that generate torsional, lateral, and longitudinal vibrations. Although the most important are torsional vibrations, all vibrations must be considered when designing a shaft system. An exact investigation of the vibrations of a shaft and propeller is dependent on the flow field and the inlet wake to the propeller, pressure fluctuations, and various shaft parameters (Batrak, 2010). These vibrations can occur throughout a ship's hull, or locally in specific parts and machinery. Therefore, there is

a large frequency range that can result in increased vibrations in the hull or in specific parts and machinery of the ship. The vibrational response of a ship's structure due to the excitation of machinery at higher frequencies can be controlled by altering the structure in local supports, such as motor foundations (Lin et al., 2009). Generally speaking, when a propeller operates behind a ship, it generates six-component oscillating loads that act on the shaft due to unsteady and non-uniform flow (Figure 1). Thus, it is important to consider the hydrodynamic added mass and damping of the propeller during unsteady flow when analyzing propeller shaft vibrations.

The shaft of a marine propulsion system extends torsional and longitudinal vibrations along the rotation axis and lateral vibrations along the transverse direction of the rotation axis. Combined, these vibrations are often referred to as general vibration modes. In the last few decades, it has been discovered that

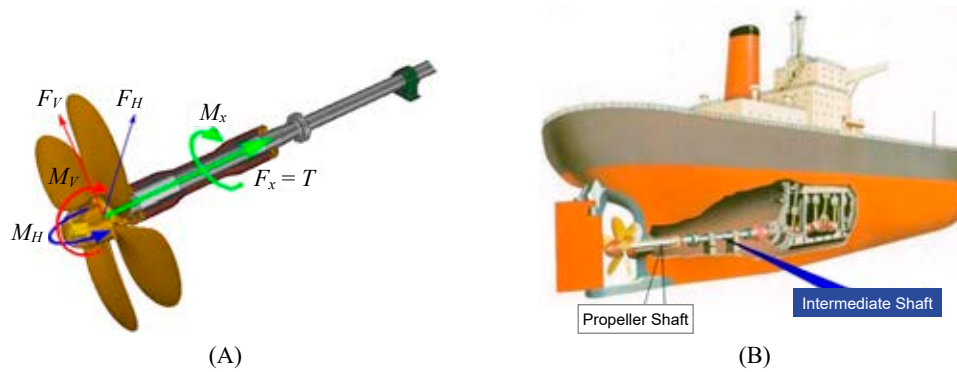


Figure 1. (A) Hydrodynamic loads acting on the propeller shaft, (B) propeller behind the ship

marine propellers (and the diesel engine's crankshaft) exhibit coupled torsional-longitudinal vibrations in the shaft system. Lateral vibrations are entirely separate from other modes.

Marine propellers operating in non-uniform currents create a vibrational response in the propeller blades which produces hydrodynamic pressure distributions and unsteady propeller shaft loads that exit the hull and cause unwanted underwater noise (Kinns et al., 2007). Due to the importance of this subject in the past, various research activities have been carried out to identify ways to reduce vibrations. The simplest methods are to increase efficiency, reduce the blade area, increase the load near the tip of the blade, and consider a large diameter at a low speed. However, reducing vibrations and noise is the first technique that a designer uses to increase the efficiency of a propeller with these methods (Bodger, Helma & Sasaki, 2016). Non-uniform inflow produces unsteady hydrodynamic forces on the blades, which causes blade vibrations. In order to predict unsteady forces in propellers that operate in non-uniform inflow, researchers have used computational fluid dynamics (He, Hong & Wang, 2012; Abbas et al., 2015; Broglia et al., 2015; Dubbioso et al., 2016).

Marine propellers operating in non-uniform incoming flows can produce very different unsteady force responses for excitation frequencies similar to the main blade frequency. Moreover, except for an increase in the unsteady forces of the propeller near resonance, blade vibration can reduce the propeller forces over a wide range of frequencies in some situations and for special propellers. This mode occurs for large hydrodynamic damping propellers and loading frequencies higher than the main propeller frequency.

By comparing the results of numerical simulations and empirical experiments, the finite element method can show the basis of the dynamics of the

shaft and also provide good technical support for predicting coupled vibrations (Huang et al., 2015). Many parameters are involved in propeller vibrations, and genetic algorithms are useful for evaluating propeller vibrations and make it possible to achieve proper efficiency and low vibration levels (Chen & Shih, 2007).

In recent years, vibrations of the shaft and propeller have become very important. Three distinct types of vibrational motion occur in marine propulsion systems, each with specific sources, features, and consequences. These three types of vibrations are: torsional, longitudinal, and lateral vibrations (Magazinović, 2009). Torsional vibrations are induced by motor torque, different propeller outputs, and the torsional elasticity of transmission systems (Murawski & Charchalis, 2014; Han, Lee & Park, 2015). In some cases, the torsional vibrational resonance of a shaft line may appear due to unusual reasons (Sestan et al., 2016). In nonlinear torsional vibrations, the shear stress in the shaft should not be ignored (Sapountzakis & Tsipiras, 2010). Parameters such as the stiffness of the joints and shaft and the damping of the connections and shaft can increase the torsional vibrations of a propeller shaft (Han, Lee & Park, 2016). In damped multi-branched gear systems, the effects of a structural damper on the torsional vibration amplitude are greater than that of a viscous damper (Firouzi et al., 2017). Longitudinal vibrations increase due to unstable propeller thrust and the relative movement between the fixed and rotary parts, which damages the thrust bearing (Zhang et al., 2014).

If flexural stiffness is ignored, errors may be generated when calculating the natural frequencies of the shaft. The prevailing vibrational mode of the propeller, which occurs during non-uniform inflow, is the fundamental flexural mode. Since shipbuilders have tended to make ships larger and larger, dynamic interactions between the hull and propulsion systems

in large-scale ships are much stronger than those in smaller ships. The deformation of a ship's hull due to excitation wave forces can affect the vibrational characteristics of propulsion systems through the bearings installed on the ship and put the reliability and safety of the propulsion system at risk (Tian et al., 2016). Stiffness and damping of the oil film of a stern tube bearing is an effective method to predict the lateral vibrational amplitude distribution along the axle.

A study of the torsional and frictional vibrations showed that the propeller is the source of vibrational excitation and can result in low-frequency noise underwater, as well as frictional noise of the shaft and its bearings (Liang & Zhao, 2014). Active control systems effectively reduce propeller shaft vibrations, and such control systems have included a pneumatic servo control that is compressed by air. Experimental results describing a controller prototype for a shaft excited by a three-blade propeller with a diameter of 0.15 m indicated that longitudinal vibrations were reduced to about 11 dB in the frequency range of 0 Hz to 10 Hz (Baz, Gilheany & Steimel, 1990). The frequency characteristics of thrust forces produced by a blade are significantly different from the total thrust force produced by all blades due to the phase cancellation of forces on various blades (Wei & Wang, 2013).

Power transmission systems with spring and damper elements can be modeled as systems with four degrees of freedom by considering all forces acting to the propeller and engine. Springs can also be placed between the main engine, the gearbox, the bearings, the propeller, and the foundation (Rao, 2005). Because of their transient nature at low speeds, resonance vibrations are not very significant. However, to prevent this phenomenon at higher speeds, the transfer of the critical speed to speeds greater than the maximum velocity, and in some vessels increased propeller weight, reducing the diameter of the shaft and adding a flexible shaft are suitable solutions (Yari & Ghassemi, 2016).

Proper evaluation of the dynamic behavior of the shaft and propeller ship is necessary to provide optional output power to the propeller and to minimize vibrations. The reliability of a propeller shaft is related to ship safety and navigation. Excessive vibrations in the torsional, longitudinal, and transverse modes and the coupling of these vibrations are undesirable and can cause damage during the operation of the shaft (Murawski, 2004). The effect of coupled torsional-longitudinal vibrations is the most significant, and designers must ensure that

the longitudinal and torsional frequencies are far apart, in order to predict the time domain when they approach each other.

Coupled longitudinal and torsional vibrations of the shaft were first discussed in 1960 using a hydrodynamic propeller with added damping and inertia, and the longitudinal and torsional vibrations were considered as coupled movements. The variation between the natural frequency obtained for the uncoupled vibration modes and the corresponding natural frequency of the coupled mode was negligible. However, the mode shapes were significantly different, and the propeller coupling can significantly affect the amplitude of vibrational forces during coupled longitudinal-torsional vibrations (Parsons, 1983). To simulate a shaft and propeller, a beam with a lumped mass model has shown good accuracy for predicting coupled vibrations (Huang et al., 2017). Thus, the main goal of this paper was to obtain the vibration equations of coupled vibrations with 4DOFs (longitudinal, lateral (horizontal and vertical), and torsional).

Propeller behind a ship

The location behind the ship where the flow into an operating propeller is non-uniform and unsteady is called the "wake field". Thus, the velocity of water in a propeller will be lower than the speed of the ship, or, on the other hand, the advance velocity (V_a) will be lower than the speed of the ship (V_S), and its relation is $V_a = V_S(1 - w)$, where w is the wake factor. The axial advance velocity V_a is important from a hydrodynamic point of view, while other the velocities (V_r and V_t) generate vibrations and noise. The advance coefficient J is defined by $J = V_a/nD$, where D and n are the diameter and rotating speed of the propeller, respectively.

Thrust forces and propeller torque at the stern of the ship are not constant and oscillating, even when the ship operates at a constant speed in still water. Since the inflow of the propeller changes with the radius, the thrust and torque oscillate, which causes an unsteady loading on the propeller blades. The main frequency of these variable forces is the same frequency of the shaft.

Typically, the components of the axial and tangential velocities (V_a and V_t) into the propeller in a single-propeller vessel vary with the relationship $r/R = 0.7$, as shown in Figure 2, where θ is the angular rotation, and V is the speed of the ship. Due to the symmetry of the ship's hull, the axial velocity should be an even function of θ , and tangential velocity

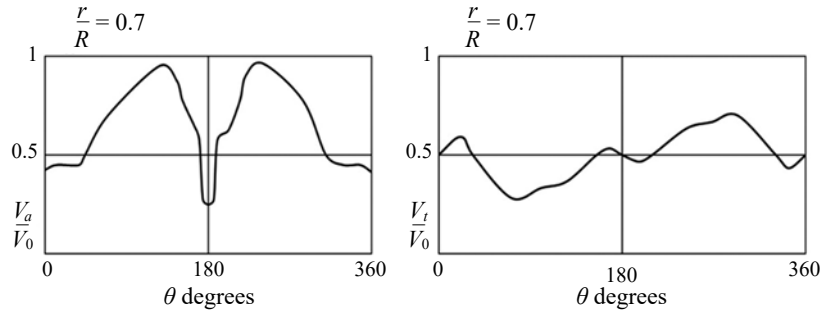


Figure 2. Axial and tangential velocities in a propeller disk (Ghose & Gokarn, 2004)

must be an odd function of θ , that is: $V_a(\theta) = V_a(-\theta)$ and $V_t(\theta) = V_t(-\theta)$.

In general, the axial and tangential velocities of a propeller disk can be expressed in terms of a Fourier series:

$$\begin{cases} V_a(r, \theta) = \sum_{m=0}^{\infty} \{a_m(r) \cos(m\theta) + b_m(r) \sin(m\theta)\} \\ V_t(r, \theta) = \sum_{m=0}^{\infty} \{a'_m(r) \cos(m\theta) + b'_m(r) \sin(m\theta)\} \end{cases} \quad (1)$$

where m is the number of harmonics that can be obtained, up to 20, to find an exact solution.

The thrust and torque at different θ values of a blade are as follows (Ghassemi, 2018; Mahmoodi, Ghassemi & Nowruzi, 2018):

$$\begin{cases} T_i = \int_{x_b}^{1.0} \frac{dT(x, \theta)}{dx} dx \\ Q_i = \int_{x_b}^{1.0} \frac{dQ(x, \theta)}{dx} dx \end{cases} \quad (2)$$

where $dT(x, \theta)$ and $dQ(x, \theta)$ are respectively the thrust and torque of a dx element in $x = r/R$ for the specified velocities $V_a(r, \theta)$ and $V_t(r, \theta)$; x_b is the dimensionless radius in the root ($x_b = r_h/R$).

The thrust and torque at θ for all of the Z blades are as follows:

$$\begin{cases} T(\theta) = \sum_{i=1}^Z T_i \left[\theta + \frac{2\pi(i-1)}{Z} \right] \\ Q(\theta) = \sum_{i=1}^Z Q_i \left[\theta + \frac{2\pi(i-1)}{Z} \right] \end{cases} \quad (3)$$

The average thrust and torque are determined by integrating the local thrust and torque along the blade range; therefore, the mean thrust and torque of a propeller are equal to:

$$\begin{cases} T = \frac{1}{2\pi} \int_0^{2\pi} T(\theta) d\theta \\ Q = \frac{1}{2\pi} \int_0^{2\pi} Q(\theta) d\theta \end{cases} \quad (4)$$

For all Z blades, the tangential force and its axial and vertical components are as follows:

$$\begin{cases} F(\theta) = \sum_{i=1}^Z F_i \left[\theta + \frac{2\pi(i-1)}{Z} \right] \\ F_H(\theta) = \sum_{i=1}^Z F_i \left[\theta + \frac{2\pi(i-1)}{Z} \right] \cos \left[\theta + \frac{2\pi(i-1)}{Z} \right] \\ F_V(\theta) = \sum_{i=1}^Z F_i \left[\theta + \frac{2\pi(i-1)}{Z} \right] \sin \left[\theta + \frac{2\pi(i-1)}{Z} \right] \end{cases} \quad (5)$$

The thrust and torque for all blades are as follows:

$$\begin{cases} T(\theta) = \sum_{i=1}^Z \sum_{m=0}^{\infty} \left\{ A_{mT} \cos \left[m\theta + \frac{2\pi(i-1)m}{Z} \right] + B_{mT} \sin \left[m\theta + \frac{2\pi(i-1)m}{Z} \right] \right\} \\ Q(\theta) = \sum_{i=1}^Z \sum_{m=0}^{\infty} \left\{ A_{mQ} \cos \left[m\theta + \frac{2\pi(i-1)m}{Z} \right] + B_{mQ} \sin \left[m\theta + \frac{2\pi(i-1)m}{Z} \right] \right\} \end{cases} \quad (6)$$

An example is shown in Figure 3 for thrust (T), torque (Q), and the vertical and horizontal forces (F_V, F_H) acting on a propeller with 4 blades. As shown in this Figure, the thrust and torque are much higher than F_V and F_H .

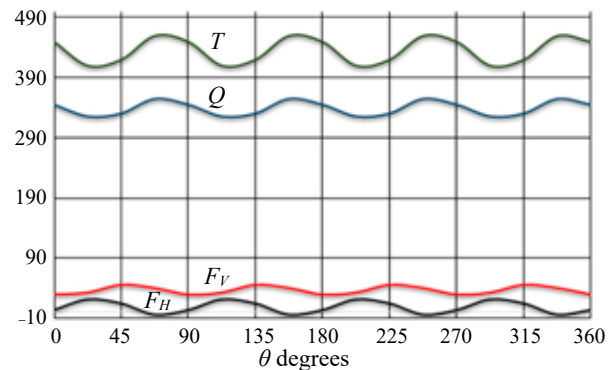


Figure 3. Oscillating propeller loading acting on the shaft

As expected, all four quantities, $T(\theta)$, $Q(\theta)$, $F_T(\theta)$, and $F_H(\theta)$ can be represented by $A + B\cos(m\theta + \varepsilon)$, where ε is the phase angle.

Added mass and added damping coefficient

Knowing the vibrational behaviors of a propeller is very important to successfully design a propulsion system. The presence of unsteady flow around a propeller that is part of the system changes the dynamic characteristics of the propeller, and therefore the interaction of the fluid and the structure should be considered in the vibration analysis of the propeller. In general, a fluid's response to additional hydrodynamic forces on a propeller is included in the added mass and damping forces. Generally, these coefficients (M_{ij} and C_{ij}) are defined in matrix form as follows:

$$M_{ij} = \begin{bmatrix} m_{11} & 0 & 0 & m_{41} & 0 & 0 \\ 0 & m_{22} & -m_{32} & 0 & m_{52} & -m_{62} \\ 0 & m_{32} & m_{33} & 0 & m_{62} & m_{52} \\ m_{41} & 0 & 0 & m_{44} & 0 & 0 \\ 0 & m_{52} & -m_{62} & 0 & m_{55} & -m_{65} \\ 0 & m_{62} & m_{52} & 0 & m_{65} & m_{66} \end{bmatrix} \quad (7)$$

$$C_{ij} = \begin{bmatrix} c_{11} & 0 & 0 & c_{41} & 0 & 0 \\ 0 & c_{22} & -c_{32} & 0 & c_{52} & -c_{62} \\ 0 & c_{32} & c_{22} & 0 & c_{62} & c_{52} \\ c_{41} & 0 & 0 & c_{44} & 0 & 0 \\ 0 & c_{52} & -c_{62} & 0 & c_{55} & -c_{65} \\ 0 & c_{62} & c_{52} & 0 & c_{65} & c_{55} \end{bmatrix} \quad (8)$$

These coefficients (m_{ij} , c_{ij}) depend on the propeller parameters like the pitch ratio (P/D), expanded area ratio (A_0/A_E), blade number (Z), water density,

and operating conditions (n , V_A), as shown in the following equation:

$$\begin{pmatrix} m_{ij} \\ c_{ij} \end{pmatrix} = f \left(\frac{A_0}{A_E}, \frac{P}{D}, Z, n, V_A, \rho \right) \quad (9)$$

Practical formulas are used to calculate these two coefficients (Carlton, 2012; Li et al., 2018).

Vibration equations

When a marine propulsion system experiences vibration, there are three different types of vibrational, each of which has specific features and consequences. These three types of vibrations are torsional, longitudinal, and lateral coupled vibrations. To derive the vibrational equations of a shaft and propeller, the shaft is considered as an equivalent cantilever beam with lumped mass at the free end.

As shown in Figure 4, the shaft is an elastic body with length L and diameter d . Other parameters such as ρ , J , L , A , and E are the density, moment of inertia, length, cross-sectional area, and Young's modulus, respectively. The other parameters m , e , and I are defined as the mass, cross-sectional eccentricity, and area moment of inertia in the axial direction, respectively.

Based on the theory of mechanics, the geometric relationship of the center-mass coordinates during transverse and longitudinal deformations, x_c and y_c , and φ , are the curvature angles as follows:

$$\begin{cases} y_c = y + e \cos \varphi \\ z_c = z + e \sin \varphi \\ \varphi = \omega t + \theta, \quad y_0 = e \cos \varphi, \quad z_0 = e \sin \varphi \end{cases} \quad (10)$$

where ω is the rotational speed, and θ is the rotation angle at the center s .

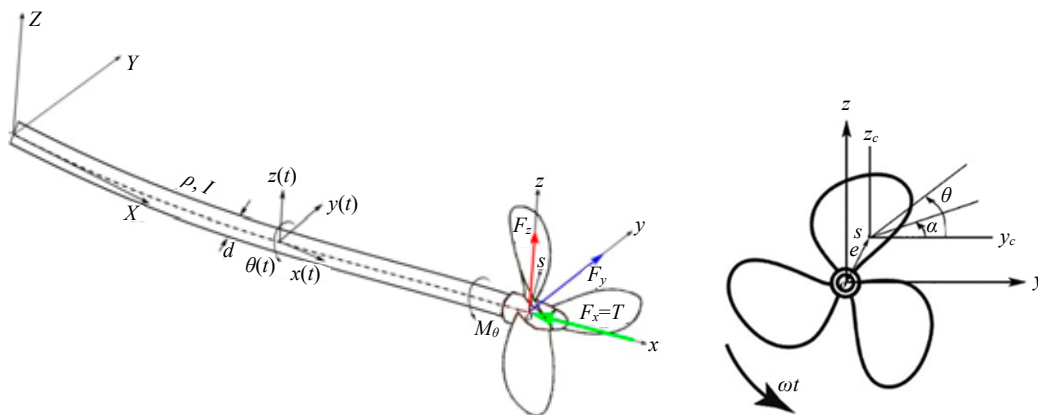


Figure 4. Shaft and propeller with an eccentricity in its cross-section

The first and second derivatives of the lateral deformation in Equation (10) are written as:

$$\begin{cases} \dot{y}_c = \dot{y} - e \dot{\varphi} \sin \varphi \\ \dot{z}_c = \dot{z} + e \dot{\varphi} \cos \varphi \\ \dot{\varphi} = \omega + \dot{\theta} \end{cases} \quad (11)$$

$$\begin{cases} \ddot{y}_c = \ddot{y} - e \ddot{\varphi} \sin \varphi - e \dot{\varphi}^2 \cos \varphi \\ \ddot{z}_c = \ddot{z} + e \ddot{\varphi} \cos \varphi - e \dot{\varphi}^2 \sin \varphi \\ \ddot{\varphi} = \ddot{\theta} \end{cases} \quad (12)$$

Torsional vibration

Torsional vibrations are created in the shaft and propeller system mainly due to the periodic injection of fuel in the diesel engine, the non-uniform rotation of the propeller, the impact of the gearbox due to gear failure, the incorrect installation of the ship's propulsion system, and the non-alignment of various parts of the shaft. The torsional vibrations of a shaft and propeller appear at different speeds of the shaft. Compared with other types of detectable vibrations, such as longitudinal or lateral vibrations, torsional vibrations are undetectable. However, this kind of shaft and propeller vibration may cause serious damage and may cause shaft failure. Torsional vibrations are characteristic of all rotary devices and equipment and are significant for internal combustion engines, shafts, and propellers. Therefore, the torsional vibration equation in the shaft and propeller system can be written as follows:

$$(J + m e^2) \ddot{\theta} + c_\theta \dot{\theta} + k_\theta \theta = M_\theta \quad (13)$$

The moment of inertia along the shaft is $J = m(D/2)^2/2$, where D represents the shaft diameter, k_θ and c_θ are the shaft's stiffness and damping coefficient, and M_θ is the moment of excitation.

Longitudinal vibration

The longitudinal vibrations of the shaft and propeller are detected by the axle in the axial direction of the shaft within its normal range. This motion may be compared with the movement of an accordion over time. Longitudinal vibrations in the shaft are mainly driven by changes in the propeller's thrust force, as well as by the forces generated by an engine's crankcase; therefore, the excitation forces resulting from the gas pressure in engine cylinders and the periodic inertia of the mass are converted

into reciprocating forces moving along the axial direction. In some cases, due to the coupled longitudinal-torsional vibrations, excessive longitudinal vibrations may be excited by an increase in torsional fluctuations.

To minimize the undesirable effects of longitudinal vibrations of a shaft, most manufacturers of low-power diesel engines install a longitudinal vibration damper inside the engine. Thus, the longitudinal vibrations of diesel engines rapidly dampen vibrations; therefore, the longitudinal vibration equation in the shaft and propeller system can be written as follows:

$$m\ddot{x} + c_x \dot{x} + k_x x = F_x \quad (14)$$

where m , c_x , k_x , and F_x are the mass, damping coefficient, longitudinal stiffness coefficient, and exciting force, respectively.

Lateral vibration

The lateral vibrations of the shaft and propeller are generated due to the lateral oscillations of parts of the shaft and propeller in a plane that passes through the center of the shaft line. The lateral vibrations are mainly excited by the propeller weight, variable induced forces of the propeller, the weight of the various parts of the shaft, and unbalances. The lateral vibration amplitude generally increases by increasing the distance between the shaft line bearings; however, a small distance between bearings can cause large lateral vibrations. Therefore, the lateral vibration equations of the shaft and propeller can be written as follows:

$$\begin{cases} m\ddot{y} + c_y \dot{y} + k_y y = F_y \\ m\ddot{z} + c_z \dot{z} + k_z z = -mg + F_z \end{cases} \quad (15)$$

where k_y and k_z are the transverse stiffness in the Y - and Z -directions, and c_y and c_z are the transverse damping coefficients. The parameters m and g are the mass and gravity of the earth.

Coupled longitudinal-torsional vibrations

When a propeller rotates behind a ship, two oscillating loads (thrust and torque) are created which are proportional to the speed and acceleration of the propeller, which couples longitudinal and torsional motions. Thus, the shaft is considered to have two degrees of freedom (2DOF), and its longitudinal contraction is excited by normal torsional motion.

This contraction mainly occurs due to a slight shaft deflection and deviation from the shaft's main axis. The shaft is shortened upon maximum contraction and shifts to its original position when the contraction is zero, so the change in the amount of contraction during each rotation causes the vibration to occur along the axial direction. The vibrational equations of this type of vibration were derived by Huang et al. (Huang et al., 2017).

$$\begin{cases} (J + m e^2) \ddot{\theta} + c_{\theta} \dot{\theta} + k_{\theta} \theta - k_{\theta x} x = T_x \sin \omega t \\ m \ddot{x} + c_x \dot{x} + k_x x - k_{x\theta} \theta = F_x \sin \omega t \end{cases} \quad (16)$$

where c_{θ} , c_x , k_{θ} , k_x , $k_{x\theta}$, and $k_{\theta x}$ are the torsional damping coefficient, the axial damping coefficient, the torsional stiffness, the axial stiffness, the coupled longitudinal-torsional stiffness, and the coupled torsional-longitudinal stiffness, respectively.

Coupled lateral-torsional vibration

Coupled transverse and torsional vibrations can occur due to a misaligned shaft, which can be caused by propeller rotation, the mass of the shaft components, the force applied to the bearings, and the encounter force of gears. In addition, the centrifugal force is appeared due to the eccentricity of propeller (Oguamanam, 2003; Shi, Xue & Song, 2010).

In the coupled torsional and lateral vibrations, the effect of the excitation forces, as well as stiffness and damping, is considered along the y - and z -axes. There are two equations for the lateral vibrations, i.e. horizontal and vertical. The coupled lateral and torsional vibration equations are defined as follows:

$$\begin{cases} m \ddot{y} + c_y \dot{y} + k_y y = \\ = m e \ddot{\theta} \sin \varphi + m e (\omega + \dot{\theta})^2 \cos \varphi + F_y \\ m \ddot{z} + c_z \dot{z} + k_z z = \\ = -m g - m e \ddot{\theta} \cos \varphi + m e (\omega + \dot{\theta})^2 \sin \varphi + F_z \\ (J + m e^2) \ddot{\theta} + c_{\theta} \dot{\theta} + k_{\theta} \theta = \\ = -m e \ddot{y} \sin \varphi + m e (g + \ddot{z}) \cos \varphi + M_{\theta} \end{cases} \quad (17)$$

The equations of motion of the shaft and propeller can be written as the matrixes (18).

Thus, it can be concluded that the eccentricity cross-section is an important parameter during coupled lateral-torsional vibrations. When $e = 0$, the widths Y and Z are independent of the torsional

$$\begin{aligned} & \begin{bmatrix} m & 0 & -m e \sin(\omega t) \\ 0 & m & m e \cos(\omega t) \\ -m e \sin(\omega t) & m e \cos(\omega t) & J + m e^2 \end{bmatrix} \begin{Bmatrix} \ddot{y} \\ \ddot{z} \\ \ddot{\theta} \end{Bmatrix} + \\ & + \begin{bmatrix} c_y & 0 & 0 \\ 0 & c_z & 0 \\ 0 & 0 & c_{\theta} \end{bmatrix} \begin{Bmatrix} \dot{y} \\ \dot{z} \\ \dot{\theta} \end{Bmatrix} + \begin{bmatrix} k_y & 0 & 0 \\ 0 & k_z & 0 \\ 0 & 0 & k_{\theta} \end{bmatrix} \begin{Bmatrix} y \\ z \\ \theta \end{Bmatrix} = \\ & = \begin{Bmatrix} m e (\omega + \dot{\theta})^2 \cos(\omega t) + F_y \\ -m g + m e (\omega + \dot{\theta})^2 \sin(\omega t) + F_z \\ + m e g \cos(\omega t) + M_{\theta} \end{Bmatrix} \quad (18) \end{aligned}$$

vibration. By increasing the eccentricity, interactions between transverse vibrations and torsional vibrations increase.

Coupled torsional-longitudinal and lateral vibrations

Without added hydrodynamic forces

In general, shaft and propeller at the stern of a ship can be affected by forces in three directions, as well as torques in three directions. Although the force component in the x -direction and the torque around the x -axis are greater than the other force and torque components, in the case of unbalanced mass, centrifugal forces can also exhibit lateral forces in the Y - and Z -directions. Therefore, the thrust force (in the x -direction), the torque around the X -axis, and the lateral forces in the Y - and Z -directions may be important as coupled torsional-longitudinal and lateral vibrations (bending moments) of the shaft and propeller.

The differential equation of vibration in the longitudinal and lateral directions and the differential equation of equilibrium in the torsion direction are expressed as follows:

$$\begin{cases} m \ddot{x} + c_x \dot{x} + k_x x - \delta k_x \theta = F_x \\ m \ddot{y} + c_y \dot{y} + k_y y = \\ = m e \ddot{\theta} \sin \phi + m e (\omega + \dot{\theta})^2 \cos \phi + F_y \\ m \ddot{z} + c_z \dot{z} + k_z z = \\ = -m g - m e \ddot{\theta} \cos \phi + m e (\omega + \dot{\theta})^2 \sin \phi + F_z \\ (J + m e^2) \ddot{\theta} + c_{\theta} \dot{\theta} + k_{\theta} \theta - \delta k_{\theta x} x = \\ = -m e \ddot{y} \sin \phi + m e (g + \ddot{z}) \cos \phi + M_{\theta} \end{cases} \quad (19)$$

The vibrational equations of the shaft and propeller without added hydrodynamic force can be written as the following matrix:

$$\begin{aligned}
 & \begin{bmatrix} m & 0 & 0 & 0 \\ 0 & m & 0 & -m \sin(\omega t) \\ 0 & 0 & m & m e \cos(\omega t) \\ 0 & -m \sin(\omega t) & m e \cos(\omega t) & J + m e^2 \end{bmatrix} \begin{Bmatrix} \ddot{x} \\ \ddot{y} \\ \ddot{z} \\ \ddot{\theta} \end{Bmatrix} + \\
 & + \begin{bmatrix} c_x & 0 & 0 & 0 \\ 0 & c_y & 0 & 0 \\ 0 & 0 & c_z & 0 \\ 0 & 0 & 0 & c_\theta \end{bmatrix} \begin{Bmatrix} \dot{x} \\ \dot{y} \\ \dot{z} \\ \dot{\theta} \end{Bmatrix} + \\
 & + \begin{bmatrix} k_x & 0 & 0 & -\delta k_x \\ 0 & k_y & 0 & 0 \\ 0 & 0 & k_z & 0 \\ -\delta k_\theta & 0 & 0 & k_\theta \end{bmatrix} \begin{Bmatrix} x \\ y \\ z \\ \theta \end{Bmatrix} = \\
 & = \begin{Bmatrix} m e (\omega + \dot{\theta})^2 \cos(\omega t) + F_y \\ -m g + m e (\omega + \dot{\theta})^2 \sin(\omega t) + F_z \\ + m e g \cos(\omega t) + M_\theta \end{Bmatrix} \quad (20)
 \end{aligned}$$

With added hydrodynamic forces

Added mass and added damping coefficients are important and effective dynamic coefficients for describing the acceleration of a body due to the non-uniform motion of a fluid around a body. These play important roles, especially in determining the control and analysis parameters of the vibration of a ship and its parts, such as the propeller. The natural frequencies of a structure in water are less than the natural frequencies in air due to the effect of the added mass of water.

The lateral forces in two directions, *Y* and *Z*, the thrust force in the *X* direction, and the torque around the *X*-axis are applied to the shaft and propeller system. So, the system has 4DOFs, and the matrix of added mass and added damping coefficients are considered as 4×4 matrices.

$$\begin{aligned}
 & \left\{ \begin{aligned}
 & (m + m_{11}) \ddot{x} + m_{41} \ddot{\theta} + (c_x + c_{11}) \dot{x} + c_{41} \dot{\theta} + \\
 & + k_x x - \delta k_x \theta = F_x \\
 & (m + m_{22}) \ddot{y} - m_{32} \ddot{z} + (c_y + c_{22}) \dot{y} - c_{32} \dot{z} + k_y y = \\
 & = (m + m_{22}) e \ddot{\theta} \sin \varphi + \\
 & + (m + m_{22}) e (\omega + \dot{\theta})^2 \cos \varphi + F_y \\
 & (m + m_{22}) \ddot{z} + m_{32} \ddot{y} + (c_z + c_{22}) \dot{z} + c_{32} \dot{y} + k_z z = \\
 & = -(m + m_{22}) g - (m + m_{22}) e \ddot{\theta} \cos \varphi + \\
 & + (m + m_{22}) e (\omega + \dot{\theta})^2 \sin \varphi + F_z \\
 & [J + (m + m_{44}) e^2] \ddot{\theta} + m_{41} \ddot{x} + (c_\theta + c_{44}) \dot{\theta} + \\
 & + c_{41} \dot{x} + k_\theta \theta - \delta k_\theta x = -(m + m_{22}) e \ddot{y} \sin \varphi + \\
 & + (m + m_{22}) e (g + \ddot{z}) \cos \varphi + M_\theta
 \end{aligned} \right. \quad (21)
 \end{aligned}$$

The vibrational equations of the shaft and propeller with added hydrodynamic forces can be written as the following matrix:

$$\begin{aligned}
 & \begin{bmatrix} m_1 & 0 & 0 & m_{41} \\ 0 & m_2 & 0 & -m_2 e \sin(\omega t) \\ 0 & 0 & m_2 & m_2 e \cos(\omega t) \\ 0 & -m_2 e \sin(\omega t) & m_2 e \cos(\omega t) & J + m_4 e^2 \end{bmatrix} \begin{Bmatrix} \ddot{x} \\ \ddot{y} \\ \ddot{z} \\ \ddot{\theta} \end{Bmatrix} + \\
 & + \begin{bmatrix} c_1 & 0 & 0 & c_{41} \\ 0 & c_2 & -c_{32} & 0 \\ 0 & c_{32} & c_3 & 0 \\ c_{41} & 0 & 0 & c_4 \end{bmatrix} \begin{Bmatrix} \dot{x} \\ \dot{y} \\ \dot{z} \\ \dot{\theta} \end{Bmatrix} + \\
 & + \begin{bmatrix} k_x & 0 & 0 & -\delta k_x \\ 0 & k_y & 0 & 0 \\ 0 & 0 & k_z & 0 \\ -\delta k_\theta & 0 & 0 & k_\theta \end{bmatrix} \begin{Bmatrix} x \\ y \\ z \\ \theta \end{Bmatrix} = \\
 & = \begin{Bmatrix} m_2 e (\omega + \dot{\theta})^2 \cos(\omega t) + F_y \\ -m_2 g + m_2 e (\omega + \dot{\theta})^2 \sin(\omega t) + F_z \\ + m_2 e g \cos(\omega t) + M_\theta \end{Bmatrix} \quad (22)
 \end{aligned}$$

where:

$$\begin{cases} m_1 = m + m_{11} & m_2 = m + m_{22} \\ m_4 = m + m_{44} & c_1 = c_x + c_{11} \\ c_2 = c_y + c_{22} & c_3 = c_z + c_{33} \\ c_4 = c_\theta + c_{44} \end{cases} \quad (23)$$

where *m_{ij}* and *c_{ij}* are defined by Eqs (7) and (8). These coefficients are important from a vibrational point of view when a propeller operates behind the ship hull. There are some practical formulas to calculate them, as given in Eq. (9), but it is difficult to determine these coefficients by numerical methods, which will be investigated in our future work.

Conclusions

In this paper, the vibration equations of the 4DOFs of the coupled torsional-longitudinal and lateral vibrations of a propeller shaft were presented. Since the propeller operates behind a ship, the flow in non-uniform and unsteady. Due to these conditions, it is important to consider the added mass, added moment of inertia, and added damping of the propeller. These terms can have effects on the vibrational response of a propulsion system. In future work, we will prepare a numerical program to solve these equations for various case studies in ship shafting systems.

References

1. ABBAS, N., KORNEV, N., SHEVCHUK, I. & ANSCHAU, P. (2015) CFD prediction of unsteady forces on marine propellers caused by the wake nonuniformity and nonstationarity. *Ocean Engineering* 104, pp. 659–672.
2. BATRAK, Y. (2010) *Torsional Vibration Calculation Issues with Propulsion Systems*. 1st IMarEST Ship Noise and Vibration Conference.
3. BAZ, A., GILHEANY, J. & STEIMEL, P. (1990) Active vibration control of propeller shafts. *Journal of Sound and Vibration* 136, 3, pp. 361–372.
4. BODGER, L., HELMA, S. & SASAKI, N. (2016) Vibration control by propeller design. *Ocean Engineering* 120, pp. 175–181.
5. BROGLIA, R., DUBBIOSO, G., DURANTE, D. & DI MASCIIO, A. (2015) Turning ability analysis of a fully appended twin screw vessel by CFD. Part I: Single rudder configuration. *Ocean Engineering* 105, pp. 275–286.
6. CARLTON, J. (2012) *Marine Propellers and Propulsion*. Butterworth-Heinemann.
7. CHEN, J.-H. & SHIH, Y.-S. (2007) Basic design of a series propeller with vibration consideration by genetic algorithm. *Journal of Marine Science and Technology* 12(3), pp. 119–129.
8. DUBBIOSO, G., DURANTE, D., DI MASCIIO, A. & BROGLIA, R. (2016) Turning ability analysis of a fully appended twin screw vessel by CFD. Part II: Single vs. twin rudder configuration. *Ocean Engineering* 117, pp. 259–271.
9. FIROUZI, J., GHASSEMI, H., AKBARI VAKILABADI, K. & KHALILNEZHAD, H. (2017) The effect of damping coefficients on the torsional vibration of the damped multi-branch gears system. *Journal of Applied Mathematics and Computational Mechanics* 16 (4), pp. 5–16.
10. GHASSEMI, H. (2018) Practical approach to calculating the hydrodynamic oscillating loads of a ship propeller under non-uniform wake field. *Scientific Journals of the Maritime University of Szczecin, Zeszyty Naukowe Akademii Morskiej w Szczecinie* 56 (128), pp. 9–20.
11. GHOSE, J.P. & GOKARN, R.P. (2004) *Basic ship propulsion*. Allied publishers.
12. HAN, H.S., LEE, K.H. & PARK, S.H. (2015) Estimate of the fatigue life of the propulsion shaft from torsional vibration measurement and the linear damage summation law in ships. *Ocean Engineering* 107, pp. 212–221.
13. HAN, H.S., LEE, K.H. & PARK, S.H. (2016) Parametric study to identify the cause of high torsional vibration of the propulsion shaft in the ship. *Engineering Failure Analysis* 59, pp. 334–346.
14. HE, X.D., HONG, Y. & WANG, R.G. (2012) Hydroelastic optimisation of a composite marine propeller in a non-uniform wake. *Ocean Engineering* 39, pp. 14–23.
15. HUANG, Q., YAN, X., WANG, Y., ZHANG, C. & WANG, Z. (2017) Numerical modeling and experimental analysis on coupled torsional-longitudinal vibrations of a ship's propeller shaft. *Ocean Engineering* 136, pp. 272–282.
16. HUANG, Q., ZHANG, C., JIN, Y., YUAN, CH. & YAN, X. (2015) Vibration analysis of marine propulsion shafting by the coupled finite element method. *Journal of Vibroengineering* 17, 7, pp. 3392–3403.
17. KINNS, R., THOMPSON, I., KESSISOGLU, N. & TSO, Y. (2007) Hull vibratory forces transmitted via the fluid and the shaft from a submarine propeller. *Ships and Offshore Structures* 2 (2), pp. 183–189.
18. LI, J., QU, Y., CHEN, Y. & HUA, H. (2018) Investigation of added mass and damping coefficients of underwater rotating propeller using a frequency-domain panel method. *Journal of Sound and Vibration* 432, pp. 602–620.
19. LIANG, X. & ZHAO, H. (2014) *Machinery vibrations induced by propeller of the ship Nomenclature*. 21st International Congress on Sound and Vibration (ICSV21), Beijing, China, pp. 1–4.
20. LIN, T.R., PAN, J., O'SHEA, P.J. & MECHEFSKE, C.K. (2009) A study of vibration and vibration control of ship structures. *Marine Structures* 22, 4, pp. 730–743.
21. MAGAZINOVIĆ, G. (2009) *Shafting Vibration Primer*. [Online] Available at: https://bib.irb.hr/datoteka/566518.Shafting_Vibration_Primer.pdf [Accessed: October 10, 2019].
22. MAHMOODI, K., GHASSEMI, H. & NOWRUZI, H. (2018) Obtaining mathematical functions of the propeller thrust and torque coefficients fluctuations at non-uniform wake flow including geometry effects. *Mechanics & Industry* 19, 205.
23. MURAWSKI, L. (2004) Axial vibrations of a propulsion system taking into account the couplings and the boundary conditions. *Journal of Marine Science and Technology* 9, pp. 171–181.
24. MURAWSKI, L. & CHARCHALIS, A. (2014) Simplified method of torsional vibration calculation of marine power transmission system. *Marine Structures* 39, pp. 335–349.
25. OGUAMANAM, D.C.D. (2003) Free vibration of beams with finite mass rigid tip load and exural – torsional coupling. *International Journal of Mechanical Sciences* 45, 6–7, pp. 963–979.
26. PARSONS, M.G. (1983) Mode Coupling in Torsional and Longitudinal Shafting Vibrations. *The Marine Technology* 20, 3, pp. 257–271.
27. RAO, T.V.H. (2005) A Diagnostic Approach to the Vibration Measurements and Theoretical Analysis of the a Dredger Propulsor System. *Journal of The Institution of Engineers*, pp. 17–23.
28. SAPOUNTZAKIS, E.J. & TSIPIRAS, V.J. (2010) Warping shear stresses in nonlinear nonuniform torsional vibrations of bars by BEM. *Engineering Structures* 32, 3, pp. 741–752.
29. SESTAN, A., VLADIMIR, N., VULIC, N. & LJUBENKOV, B. (2012) A study into resonant phenomena in the catamaran ferry propulsion system. *Transactions of FAMENA* 36 (1), pp. 35–44.
30. SHI, L., XUE, D. & SONG, X. (2010) Research on shafting alignment considering ship hull deformations. *Marine Structures* 23, 1, pp. 103–114.
31. TIAN, Z., YAN, X.P., ZHANG, C., XIONG, Y.-P. & YANG, P. (2016) Vibration characteristics analysis on ship propulsion system taking hull deformations into account. *Technical gazette* 23, 3, pp. 783–790.
32. WEI, Y. & WANG, Y. (2013) Unsteady hydrodynamics of blade forces and acoustic responses of a model scaled submarine excited by propeller's thrust and side-forces. *Journal of Sound and Vibration* 332, 8, pp. 2038–2056.
33. YARI, E. & GHASSEMI, H. (2016) Free and Forced Vibrations of a Shaft and Propeller Using the Couple of Finite Volume Method, Boundary Element Method and Finite Element Method. *Ravish/hā-yi ādadī dar Muhandisī* 34(2), pp. 13–36 (in Persian).
34. ZHANG, G., ZHAO, Y., LI, T. & ZHU, X. (2014) Propeller Excitation of Longitudinal Vibration Characteristics of Marine Propulsion Shafting System. *Shock and Vibration* 413592.